Analyst

COMMUNICATION

View Article Online
View Journal | View Issue

Cite this: *Analyst*, 2025, **150**, 4925

Received 6th August 2025,
Accepted 29th September 2025

DOI: 10.1039/d5an00839e

rsc.li/analyst

Detection of carbapenemase-mediated antimicrobial resistance using surface-enhanced Raman scattering

Ziying Wang,†[a] Hridaynath Bhattacharjee, †[a] Mitchell A. Jeffs, †[b] Rachel A. V. Gray,[b] Yazan Bdour,[a] Aristides Docoslis,[a] Christopher T. Lohans *[b] and Carlos Escobedo *[a]

Antimicrobial resistance (AMR) poses a significant global health threat, necessitating rapid and precise detection methods. One widespread mechanism of AMR involves bacterial production of β-lactamase enzymes which render β-lactam antibiotics ineffective. The ability of β-lactamases with carbapenemase activity to degrade carbapenems, β-lactams used as antibiotics of last resort, is of particular concern. Carbapenemase-producing organisms (CPOs) cause infections with high mortality rates, hence, their timely detection is of utmost importance. Here, we applied surface-enhanced Raman scattering (SERS) to the detection of carbapenemase activity, where our data reveal that enzyme-catalyzed carbapenem hydrolysis results in distinct spectral fingerprint changes. We capitalize on this finding by illustrating an experimental methodology implementing SERS that permits the detection of CPOs.

Antimicrobial resistance (AMR) poses a growing threat to public health around the world and puts a substantial financial strain on global healthcare systems.[1] It is widely acknowledged that the excessive and irresponsible use of antibiotics has significantly contributed to the emergence of resistant bacterial strains.[2,3] β-Lactams, including penicillins, cephalosporins, carbapenems, and monobactams, are the most prescribed antibiotics globally.[4] Carbapenems are potent antibiotics used for many indications, including urinary tract infections, pneumonia, intra-abdominal infections, meningitis, and in some cases, they are considered the last resort for targeting multidrug resistant pathogens.[5] However, these antibiotics can be hydrolysed by β-lactamase enzymes which have carbapenemase activity. Carbapenemase-producing organisms (CPOs) include *Escherichia coli*, *Pseudomonas aeruginosa*, *Acinetobacter baumannii*, *Klebsiella pneumoniae*, and *Enterobacter cloacae*.[6,7] CPO infections have high mortality rates,[7–9] hence, timely and accurate detection of such resistant microorganisms is crucial to initiate appropriate antimicrobial therapy and implement infection prevention and control measures.[10,11] However, many conventional techniques for detecting CPOs are either time-consuming, expensive, and/or labor-intensive.[12–14] Containing these health concerns is extremely challenging without diagnostic assays capable of time-efficient and reliable pathogen characterization.[15] Amongst other methods, recent advances in microfluidics,[16,17] surface plasmon resonance,[18] electrochemical biosensing,[19,20] immunodetection,[21,22] and isothermal nucleic acid amplification technology[23] have led to innovative systems with the potential to transform AMR detection.

Surface-enhanced Raman scattering (SERS) is a technique that combines Raman spectroscopy with plasmonic effects. It amplifies excitation and scattering processes, resulting in signal enhancement that makes it suitable for ultrasensitive chemical analysis.[24,25] Its high sensitivity, narrow spectral peaks, rapid operation, and ability to function under ambient conditions make it promising for studying complex biological systems.[26] Silver or gold nanoparticles supported on paper are often used as SERS substrates and their popularity is on the rise in chemical analysis due to affordability, portability, and ease of use.[27,28] However, the potential of SERS as a rapid surveillance technology for tracking the emergence and spread of antimicrobial resistance remains largely unexplored.[29–34] Reports describing the use of paper-based SERS substrates for the detection of AMR are even scarcer.[35] The development of point-of-care devices that are rapid, cost-effective, portable, and do not necessitate specialized training is of paramount importance, particularly during deployment in resource-constrained settings.

In this work, we present the successful rapid identification of carbapenemase-producing bacteria using a commercially available paper-based SERS-active substrate.[37] In the presence

[a]*Department of Chemical Engineering, Queen's University, Kingston, ON K7L 3N6, Canada. E-mail: carlos.escobedo@queensu.ca*
[b]*Department of Biomedical and Molecular Sciences, Queen's University, Kingston, ON K7L 3N6, Canada. E-mail: christopher.lohans@queensu.ca*
† These authors contributed equally.

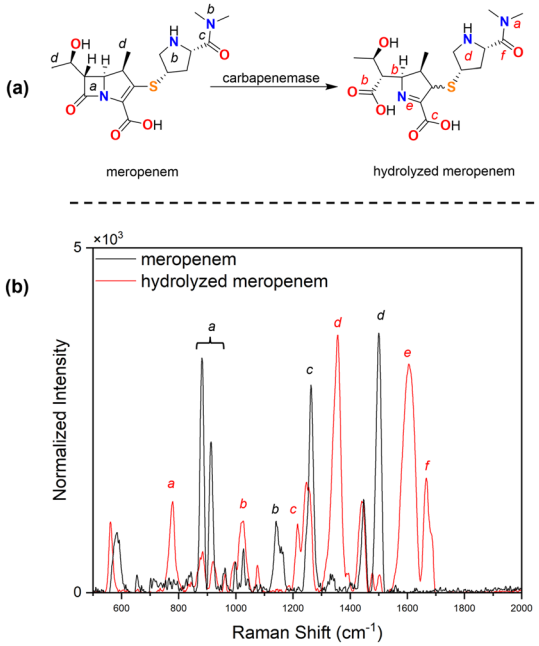

Fig. 1 (a) Reaction scheme showing the carbapenemase-catalysed degradation of the carbapenem meropenem. (b) SERS spectra of meropenem and the meropenem-derived hydrolysis product generated by the carbapenemase KPC-2. The imine tautomer of the hydrolysis product is expected to be the major meropenem-derived species that is present.[36] Characteristic peaks of meropenem and hydrolysed meropenem are marked in black and red letters, respectively.

of a carbapenemase, the carbapenem β-lactam ring is broken open, generating a hydrolysis product (Fig. 1a).[36,38] We explored the application of SERS to detect these chemical alterations.

First, we obtained the SERS spectrum of the carbapenem meropenem (in black, Fig. 1b) and assigned some of its characteristic peaks. The SERS peaks observed at 880 and 914 cm^{-1} in meropenem correlate to the β-lactam ring (marked *a* in black, Fig. 1b).[39–41] The other distinctive peaks at 1143, 1250, and 1500 cm^{-1} (marked *b*, *c*, *d* in black) can be attributed to C–N in the pyrrolidine ring, C–N in the dimethylcarbamoyl group, and aliphatic C–H in general, respectively.[39–42] A detailed list of identified peaks is shown in Table S1 (SI).

Next, we compared the SERS spectrum of meropenem with the meropenem-derived hydrolysis product formed following incubation with carbapenemase enzymes (Scheme 1). We obtained the meropenem hydrolysis product at a concentration of 10 mg L^{-1} using purified carbapenemase enzymes (see SI for details). We tested two major carbapenemases in this study: KPC-2 and OXA-48; results obtained from KPC-2 are discussed below, and those from OXA-48 can be found in the SI. The SERS spectrum of the meropenem hydrolysis product is displayed in Fig. 1b (in red) and shows distinct differences from the original meropenem spectrum. Peaks that are unique to the hydrolysis product are marked with red letters (Fig. 1b). Peaks at 780, 1077, 1217, and 1356 cm^{-1} appear exclusively in the spectrum for hydrolysed meropenem and were assigned to C–N in the dimethylcarbamoyl group, C–H in the hydroxyethyl group, C–O–H in a carboxylic acid, and C–H on the pyrrolidine ring, respectively.[39,40] One of the significant findings from this analysis is the appearance of the peak at ~1600 cm^{-1} (marked *e* in red), which was assigned to the C=N bond in the pyrroline ring of the hydrolysed product (see Fig. 1a).[43] The band at ~1670 cm^{-1} (marked *f* in red), as well, is unique to the hydrolysed meropenem and was assigned to the amide I vibrational mode (C=O stretching of amide group).[44] These unambiguous differences between the spectral fingerprints of meropenem and its hydrolysis product confirm the chemical transformation of meropenem by KPC-2, highlighting the ability of SERS to detect subtle molecular changes.

Fig. 2 presents a time course of SERS spectra acquired for KPC-2 and meropenem 5 min and 20 min after mixing the components. Peaks corresponding to the hydrolysis product (highlighted in green) became more prominent, while the intensity of peaks related to meropenem (highlighted in red) decreased over time. A prominent peak at 1450 cm^{-1} showed significantly higher intensity at both the 5 and 20 min intervals. This could be due to the C–N stretching from the enamine tautomer of the hydrolysed product,[36,39] as well as the C–N stretching in the amide bonds of KPC-2.[45] Some peaks align with previously reported SERS data of KPC-2 (see Table S2).[45] We obtained similar results when meropenem was treated with OXA-48 (see Fig. S3 and S4 in the SI).

Principal component analysis (PCA) of SERS signals of meropenem alone and when combined with KPC-2, covering 200–3200 cm^{-1}, extracted the first two principal components accounting for 98.5% variance (see Fig. S5 in SI). The score plot clearly separated the samples, suggesting effective differentiation of the spectra and reflecting chemical changes in meropenem resulting from its hydrolysis by KPC-2. Similar PCA results were obtained when OXA-48 was tested (Fig. S6). In the absence of a carbapenemase, however, the meropenem spectrum remained unchanged in aqueous solution for several days at room temperature (see Fig. S7).[41]

The bioassay was subsequently tested using bacterial cells to evaluate its potential for clinical applications. First, SERS spectra were acquired for a mixture of meropenem and an *E. coli* strain that does not produce carbapenemases (Fig. 3a). The characteristic peaks from the β-lactam ring of meropenem marked with black dotted lines remain unchanged. Additionally, the peaks expected from the hydrolysed product were not observed (marked with red dotted lines). However, the spectrum appears more complex, likely due to *E. coli*-derived products present in the mixture.[46] When meropenem was mixed with KPC-2-producing *E. coli*, spectral changes were seen (Fig. 3b). Peaks at 1217, 1356, and 1605 cm^{-1} are consistent with the hydrolysis of meropenem in the presence of the carbapenemase-producing *E. coli*. Disappearance of peaks related to β-lactam ring further confirms the hydrolysis of meropenem and potency

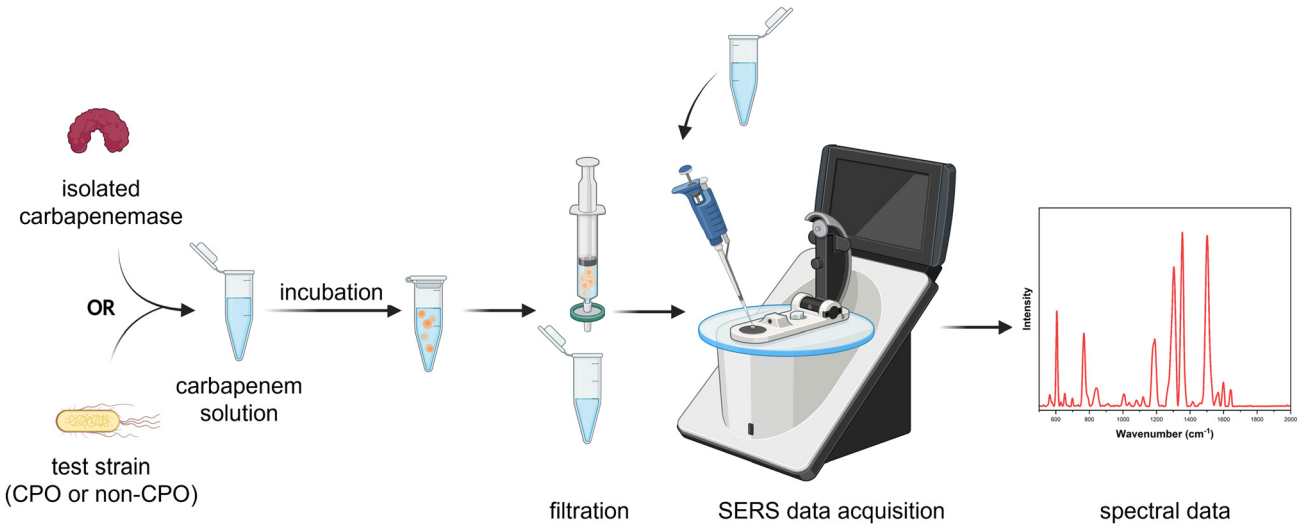

Scheme 1 Experimental workflow of the assay.

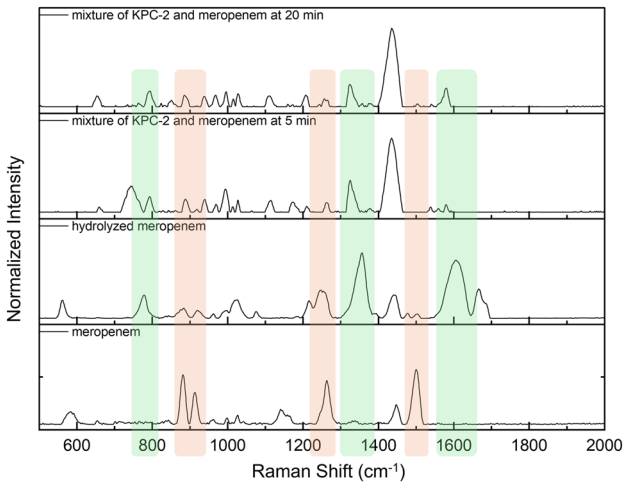

Fig. 2 Monitoring a mixture of meropenem and KPC-2 at different time points using SERS. Red bands highlight the disappearing peaks of meropenem, while green bands indicate the emergence of new peaks corresponding to its hydrolysis product.

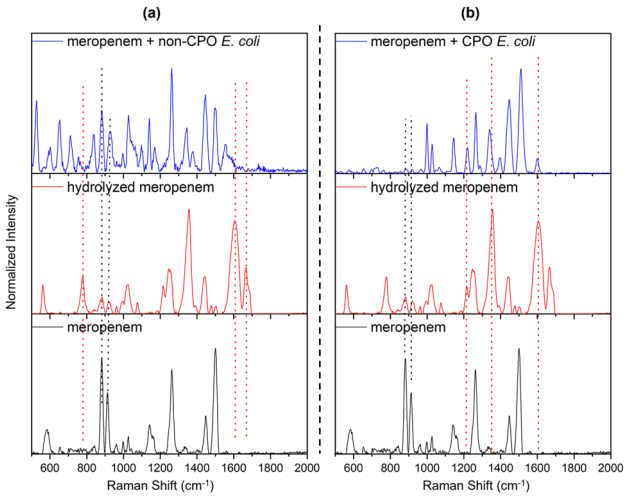

Fig. 3 (a) SERS spectrum of meropenem (in blue) following treatment with an *E. coli* strain that does not produce a carbapenemase. Spectra of meropenem and its hydrolysed product are shown (in black and red, respectively) for comparison. (b) SERS spectrum of meropenem (in blue) when treated with a KPC-2-producing *E. coli* strain. Spectra of meropenem and its hydrolysed product are shown (in black and red, respectively) for comparison. Note that, within the timeframe of the assay, many of the cells of the meropenem-susceptible non-CPO strain had likely not yet been killed.[50]

of the CPO *E. coli* used (black dotted lines in Fig. 3b). Moreover, the decreased intensities of the peaks that were attributed to *E. coli* products, when compared to Fig. 3a, may reflect the survival of the *E. coli* following antibiotic treatment. The results obtained with SERS are consistent with UV-Vis spectrophotometric detection assay of meropenem hydrolysis, a known antimicrobial susceptibility test (Fig. S8).[47] Overall, these observations confirm that SERS can be effectively applied to the measurement of meropenem hydrolysis by CPOs. However, the positive detection of meropenem hydrolysis by a CPO depends on the catalytic efficiency and the amount of the carbapenemase produced by the strain. More CPO cells are needed to detect a strain producing a weak carbapenemase.[48,49]

Conclusions

In summary, we have demonstrated that clinically relevant carbapenemase-producing bacteria can be detected by means of SERS. By analysing spectral changes in meropenem before and after its degradation either by purified carbapenemase enzymes or carbapenemase-producing bacteria, we discovered that the hydrolysis of meropenem resulted in distinct changes to the spectral fingerprint. Moreover, we developed an experimental protocol that can form the foundation of future clinical

tests used to identify resistant bacteria *in situ* and in real time. We are currently exploring alternative SERS-active substrates[51,52] and more advanced sampling methodologies that can further improve the detection sensitivity and discriminatory ability of our approach. We strive to employ SERS for testing CPO strains originating from intricate sample matrices, such as blood, saliva, and wastewater. In these cases, the quantity of carbapenemase production is uncertain or the specific type of carbapenemase is unknown. To address these challenges, we plan to utilize supervised machine learning (ML) algorithms, which have been proven to enhance accuracy by identifying spectral changes, recognizing patterns, and effectively managing large datasets.[26,53,54] Owing to its potential for ultrasensitive, time-efficient, and point-of-need detection, SERS lends itself to the development of diagnostic methods that permit timely selection of antibiotics and implementation of infection prevention and control measures, thus reducing the disease burden associated with AMR.

Author contributions

Z. W.: writing – original draft, software, methodology, investigation, data curation. H. B.: writing – original draft, writing – review & editing, investigation, data curation, formal analysis, visualization. M. A. J.: investigation, data curation, formal analysis. R. A. V. G.: investigation, data curation. Y. B.: supervision. A. D.: writing – review & editing, supervision, funding acquisition. C. E.: supervision, writing – review & editing resources, conceptualization, funding acquisition. C. T. L.: writing – review & editing, supervision, resources, conceptualization, funding acquisition.

Conflicts of interest

There are no conflicts to declare.

Data availability

The data supporting the findings of this study are available within the article or its supplementary information (SI). Supplementary information is available. See DOI: https://doi.org/10.1039/d5an00839e.

Acknowledgements

We thank financial support from the Natural Sciences and Engineering Research Council of Canada (Discovery Grant, CE, RGPIN-2019-04292, and AD, RGPIN-2018-05138; RTI Grant, AD, RTI-2023-00399), Canada Foundation for Innovation, CE, 319670, and the Canadian Tri-Agency New Frontiers in Research Fund, CTL, NFRF-2021-01035.

References

1 M. A. Salam, M. Y. Al-Amin, M. T. Salam, J. S. Pawar, N. Akhter, A. A. Rabaan and M. A. A. Alqumber, *Healthcare*, 2023, **11**, 1946.
2 R. Chopra, G. Alderborn, F. Podczeck and J. M. Newton, *Int. J. Pharm.*, 2002, **239**, 171–178.
3 S. B. Zaman, M. A. Hussain, R. Nye, V. Mehta, K. T. Mamun and N. Hossain, *Cureus*, 2017, **9**, e1403.
4 K. Bush and P. A. Bradford, *Cold Spring Harb. Perspect Med.*, 2016, **6**, a025247.
5 C. M. Baldwin, K. A. Lyseng-Williamson and S. J. Keam, *Drugs*, 2008, **68**, 803–838.
6 R. A. Bonomo, E. M. Burd, J. Conly, B. M. Limbago, L. Poirel, J. A. Segre and L. F. Westblade, *Clin. Infect. Dis*, 2018, **66**, 1290–1297.
7 S. Mariappan, U. Sekar and A. Kamalanathan, *Int. J. Appl. Basic Med. Res.*, 2017, **7**, 32–39.
8 M. S. Baek, J. H. Kim, J. H. Park, T. W. Kim, H. I. Jung and Y. S. Kwon, *Sci. Rep.*, 2024, **14**, 597.
9 L. Xu, X. Sun and X. Ma, *Ann. Clin. Microbiol. Antimicrob.*, 2017, **16**, 18.
10 D. Yamin, V. Uskokovic, A. M. Wakil, M. D. Goni, S. H. Shamsuddin, F. H. Mustafa, W. A. Alfouzan, M. Alissa, A. Alshengeti, R. H. Almaghrabi, M. A. A. Fares, M. Garout, N. A. Al Kaabi, A. A. Alshehri, H. M. Ali, A. A. Rabaan, F. A. Aldubisi, C. Y. Yean and N. Y. Yusof, *Diagnostics*, 2023, **13**, 3246.
11 H. Wang, C. Jia, H. Li, R. Yin, J. Chen, Y. Li and M. Yue, *Front. Mol. Biosci.*, 2022, **9**, 976705.
12 A. Vasala, V. P. Hytonen and O. H. Laitinen, *Front. Cell. Infect. Microbiol.*, 2020, **10**, 308.
13 G. D. Kaprou, I. Bergspica, E. A. Alexa, A. Alvarez-Ordonez and M. Prieto, *Antibiotics*, 2021, **10**, 209.
14 J. Hassall, C. Coxon, V. C. Patel, S. D. Goldenberg and C. Sergaki, *npj Antimicrob. Resist.*, 2024, **2**, 16.
15 F. Ramírez-Castillo, A. Loera-Muro, M. Jacques, P. Garneau, F. Avelar-González, J. Harel and A. Guerrero-Barrera, *Pathogens*, 2015, **4**, 307–334.
16 K. E. Mach, R. Mohan, E. J. Baron, M. C. Shih, V. Gau, P. K. Wong and J. C. Liao, *J. Urol.*, 2011, **185**, 148–153.
17 A. M. Shuppara, G. C. Padron, A. Sharma, Z. Modi, M. D. Koch and J. E. Sanfilippo, *Sci. Adv.*, 2025, **11**, eads5005.
18 J. Hu, M. Ghosh, M. J. Miller and P. W. Bohn, *Anal. Methods*, 2019, **11**, 296–302.
19 H. Ceylan Koydemir, H. Kulah, C. Ozgen, A. Alp and G. Hascelik, *Biosens. Bioelectron.*, 2011, **29**, 1–12.
20 L. Xu, W. Liang, Y. Wen, L. Wang, X. Yang, S. Ren, N. Jia, X. Zuo and G. Liu, *Biosens. Bioelectron.*, 2018, **99**, 424–430.
21 N. Bhardwaj, S. K. Bhardwaj, J. Mehta, G. C. Mohanta and A. Deep, *Anal. Biochem.*, 2016, **505**, 18–25.
22 N. Gupta, V. Renugopalakrishnan, D. Liepmann, R. Paulmurugan and B. D. Malhotra, *Biosens. Bioelectron.*, 2019, **141**, 111435.
23 M. Feldgarden, V. Brover, D. H. Haft, A. B. Prasad, D. J. Slotta, I. Tolstoy, G. H. Tyson, S. Zhao, C. H. Hsu,

P. F. McDermott, D. A. Tadesse, C. Morales, M. Simmons, G. Tillman, J. Wasilenko, J. P. Folster and W. Klimke, *Antimicrob. Agents Chemother.*, 2019, **63**, e00483–19.
24 E. C. Le Ru and B. Auguie, *ACS Nano*, 2024, **18**, 9773–9783.
25 C. Zong, M. Xu, L. J. Xu, T. Wei, X. Ma, X. S. Zheng, R. Hu and B. Ren, *Chem. Rev.*, 2018, **118**, 4946–4980.
26 L. L. Lin, R. Alvarez-Puebla, L. M. Liz-Marzan, M. Trau, J. Wang, L. Fabris, X. Wang, G. Liu, S. Xu, X. X. Han, L. Yang, A. Shen, S. Yang, Y. Xu, C. Li, J. Huang, S. C. Liu, J. A. Huang, I. Srivastava, M. Li, L. Tian, L. B. T. Nguyen, X. Bi, D. Cialla-May, P. Matousek, N. Stone, R. P. Carney, W. Ji, W. Song, Z. Chen, I. Y. Phang, M. Henriksen-Lacey, H. Chen, Z. Wu, H. Guo, H. Ma, G. Ustinov, S. Luo, S. Mosca, B. Gardner, Y. T. Long, J. Popp, B. Ren, S. Nie, B. Zhao, X. Y. Ling and J. Ye, *ACS Appl. Mater. Interfaces*, 2025, **17**, 16287–16379.
27 A. Laliwala, A. Pant, D. Svechkarev, M. R. Sadykov and A. M. Mohs, *npj Biosens.*, 2024, **1**, 17.
28 F. Mazur, A. D. Tjandra, Y. Zhou, Y. Gao and R. Chandrawati, *Nat. Rev. Bioeng.*, 2023, **1**, 180–192.
29 Z. Al-Shaebi, F. Uysal Ciloglu, M. Nasser and O. Aydin, *ACS Omega*, 2022, **7**, 29443–29451.
30 S. Das, K. Saxena, J. C. Tinguely, A. Pal, N. L. Wickramasinghe, A. Khezri, V. Dubey, A. Ahmad, V. Perumal, R. Ahmad, D. N. Wadduwage, B. S. Ahluwalia and D. S. Mehta, *ACS Appl. Mater. Interfaces*, 2023, **15**, 24047–24058.
31 S. Singh, D. Kumbhar, D. Reghu, S. J. Venugopal, P. T. Rekha, S. Mohandas, S. Rao, A. Rangaiah, S. K. Chunchanur, D. K. Saini and S. Umapathy, *Anal. Chem.*, 2022, **94**, 14745–14754.
32 S. Singh, T. Verma, B. Khamari, E. P. Bulagonda, D. Nandi and S. Umapathy, *Anal. Chem.*, 2023, **95**, 11342–11351.
33 W. Wang and P. J. Vikesland, *Environ. Sci. Technol.*, 2023, **57**, 13375–13383.
34 X. Yi, Y. Song, X. Xu, D. Peng, J. Wang, X. Qie, K. Lin, M. Yu, M. Ge, Y. Wang, D. Zhang, Q. Yang, M. Wang and W. E. Huang, *Anal. Chem.*, 2021, **93**, 5098–5106.
35 S. H. Hilton, C. Hall, H. T. Nguyen, M. L. Everitt, P. DeShong and I. M. White, *Anal. Chim. Acta*, 2020, **1127**, 207–216.
36 C. T. Lohans, E. I. Freeman, E. V. Groesen, C. L. Tooke, P. Hinchliffe, J. Spencer, J. Brem and C. J. Schofield, *Sci. Rep.*, 2019, **9**, 13608.
37 https://www.oceanoptics.com/accessories/sampling-accessories/.
38 C. T. Lohans, E. van Groesen, K. Kumar, C. L. Tooke, J. Spencer, R. S. Paton, J. Brem and C. J. Schofield, *Angew. Chem., Int. Ed.*, 2018, **57**, 1282–1285.
39 S. Muneer, D. K. Sarfo, G. A. Ayoko, N. Islam and E. L. Izake, *Nanomaterials*, 2020, **10**, 1756.
40 J. Cielecka-Piontek, M. Paczkowska, K. Lewandowska, B. Barszcz, P. Zalewski and P. Garbacki, *Chem. Cent. J.*, 2013, **7**, 98.
41 S. Jaruratanasirikul and S. Sriwiriyajan, *Southeast Asian J. Trop. Med. Public Health*, 2003, **34**, 627–629.
42 V. P. Anjos, C. Marangoni, R. Nadas, T. N. Machado, D. Krul, L. S. Rodrigues, L. M. Dalla-Costa, W. H. Schreiner, D. M. Zezell, A. G. Bezerra Jr. and R. E. de Goes, *Antibiotics*, 2024, **13**, 1157.
43 C. Liu, C. Franceschini, S. Weber, T. Dib, P. Liu, L. Wu, E. Farnesi, W. S. Zhang, V. Sivakov, P. B. Luppa, J. Popp and D. Cialla-May, *Talanta*, 2024, **271**, 125697.
44 D. Kurouski, T. Postiglione, T. Deckert-Gaudig, V. Deckert and I. K. Lednev, *Analyst*, 2013, **138**, 1665–1673.
45 G. Guo, C. Guo, X. Qie, D. He, S. Meng, L. Su, S. Liang, S. Yin, G. Yu, Z. Zhang, X. Hua and Y. Song, *Spectrochim. Acta, Part A*, 2024, **308**, 123699.
46 D. Yang, H. Zhou, C. Haisch, R. Niessner and Y. Ying, *Talanta*, 2016, **146**, 457–463.
47 J. G. Routsias, D. Tsakogiannis, M. Katsiki, D. Marinou, M. Mavrouli, G. Vrioni and A. Tsakris, *Int. J. Antimicrob. Agents*, 2020, **56**, 106211.
48 S. C. Mehta, I. M. Furey, O. A. Pemberton, D. M. Boragine, Y. Chen and T. Palzkill, *J. Biol. Chem.*, 2021, **296**, 100155.
49 V. Stojanoski, L. Hu, B. Sankaran, F. Wang, P. Tao, B. V. V. Prasad and T. Palzkill, *ACS Infect. Dis.*, 2021, **7**, 445–460.
50 M. Mora-Ochomogo, M. A. Jeffs, J. L. Liu and C. T. Lohans, *RSC Chem. Biol.*, 2025, DOI: 10.1039/d5cb00092k.
51 S. Azimi and A. Docoslis, *Sens. Actuators, B*, 2023, **393**, 134250.
52 S. Azimi, M. Moridsadat, B. Shastri, B. W. Banfield, C. Escobedo and A. Docoslis, *Sens. Actuators Rep.*, 2025, **9**, 100273.
53 S. X. Leong, L. K. Koh, C. S. L. Koh, G. C. Phan-Quang, H. K. Lee and X. Y. Ling, *ACS Appl. Mater. Interfaces*, 2020, **12**, 33421–33427.
54 S. X. Leong, Y. X. Leong, E. X. Tan, H. Y. F. Sim, C. S. L. Koh, Y. H. Lee, C. Chong, L. S. Ng, J. R. T. Chen, D. W. C. Pang, L. B. T. Nguyen, S. K. Boong, X. Han, Y. C. Kao, Y. H. Chua, G. C. Phan-Quang, I. Y. Phang, H. K. Lee, M. Y. Abdad, N. S. Tan and X. Y. Ling, *ACS Nano*, 2022, **16**, 2629–2639.